Evaluation of Ferruginous materials, Twin Rivers, Zambia

Summary

Four submitted samples of lump iron ore, previously identified as haematite and limonite and tentatively interpreted as laterite were examined petrographically and geochemically. Only one of these specimens was confirmed as being laterite, with two being haematitic iron ores with a replacement texture, and the fourth a specularite.

Ochre impregnation from a supposed hammerstone was sampled and analysed geochemically. Although there was no positive correlation between the ochre and any of the lump samples, the overall chemical composition made a derivation from the laterite unlikely, with the similarity with the specularite being strongest.

Further investigation of the possible origin of the ochreous material was made through examination of the matrix and of a clast from the breccia. The carbonate clast proved not to be likely source material for ochre, and the matrix proved to be very highly phosphatic, rather than ferruginous.

A specimen suspected as being marked by sets of sub-parallel scratches was cut in an unsuccessful attempt to produce a thin section. The lithology was extremely soft and powdered on cutting. The cut surface clearly showed, however, a crack marked by iron oxides, parallel to the supposed scratches. This makes it extremely likely the “scratches” are natural enlargements of these cracks during weathering.

Introduction

A variety of samples from the Twin Rivers site were examined for evidence concerning the origin of the ferruginous materials.

Sampling included one specimens identified as “limonite” (TR96 Block F limonite: TR1) and three specimens identified as laterite (laterites #2-4: TR2-4). Ochre was collected from the surface of a probable hammerstone (TR5) and ochreous-appearing material from the matrix of a breccia specimen (TR6). Samples were also taken from the reverse of a block showing marks previously interpreted as scratches (TR7) and from a clast within the breccia (TR8) for examination as polished blocks.

Analyses and investigations taken are listed below:

sample	*XRF: major elements*	*ICP-MS : trace elements*	*Polished block for SEM*
TR1	X	X	X
TR2	X	X	X
TR3	X	X	X
TR4	X	X	X
TR5		X	
TR6	X	X	X
TR7			Abandoned
TR8			X

The iron ore specimens were texturally divisible into laterite (TR1), replacement iron ores (TR2, TR4) and specularite (TR3).

Description of the iron ore lump specimens

TR1 (labelled: TR96 Block F limonite)

This sample comprises a brown pebble approximately 4cm in diameter, which is partly coated in a dark brown ferruginous rind, resembling desert varnish. The rock appears to comprise well-lithified, ferruginous particles 1-2cm across, with softer, more silty areas between.

The polished block shows that the rock contains silt- and sand-grade grains (20 – 1000μm) of quartz, feldspar and mica (Figure 1a-b), in a fine-grained matrix dominated by iron oxides. The micas show little evidence of penetrative alteration, but have a sharp contact with the enclosing iron oxides (Figure 1a). The iron rich groundmass shows a variable backscatter coefficient, with amorphous areas (20-80μm across) of greater electron density probably representing areas of anhydrous haematite in an otherwise dominantly hydrate (goethite?) material (Figure 1c-d). Some of the haematitic patches show small (sub-micron) grains of cerium-rich phosphate (monazite?; Figure 1d). There are some examples of ferruginous coated grains of up to 200μm (Figure 1e), but these are uncommon. The brown coating on the pebble was apparently clay-rich (Figure 1f).

TR2 (labelled: Twin Rivers 96, east wall solution cavity)

This sub-angular pebble, 6 cm maximum diameter, is dominantly hard and very dark. It is traversed by a vein and a tubular structure, containing saccharoidal quartz. One end of the pebble presents a delicate mesh-like structure suggesting dissolution of an originally abutting mineral phase (possibly carbonate or sulphide).

The polished section shows this sample bears a network of quartz (Figure 1g), apparently marking the boundaries of a former grain texture, with the original grains 50-1000μm in diameter. The grain boundaries may be marked by discontinuous rims of quartz (Figure 1g-i), discontinuous rims of haematite(Figure 1i), or discrete neomorphic quartz grains (which may show intergrown haematite; Figure 1h). In some areas of the section, variation in the haematite produces a concentrically laminated structure (Figure 1j).

TR3 (labelled: Twin Rivers 96, east wall solution cavity, haematite)

This sample is a rounded pebble 6cm maximum diameter, with a brown, polished surface coating resembling desert varnish. This is a specimen of coarse specularite, with substantial porosity, some of which is occluded by a fine-grained white material.

The main generation of haematite crystals range up to 1000μm in length, and 25μm in width(Figure 1k-n). These are coated by a second generation, oriented approximately normal to the surface of the first, and just a few microns in length (Figure 1m). The main generation of crystals are arranged randomly, or in sheaves of crystals up to 1000μm across (Figure 1n). In some areas these sheaves are arranged in a crudely radial arrangement.

The whole structure is highly porous, but large pores up to 1000μm across may be largely occluded by aluminous material, including kaolinite, alumina and iron aluminium silicates (Figure 1l). Adjacent to these pores the haematite may be overgrown by a very fine-grained mineral containing Mn and Al, locally with some Ti (e.g. Figure 1m, lower left). This phase is too fine-grained to obtain a meaningful microanalysis, but the composition would be compatible with the Mn-Al spinel galaxite.

TR4 (labelled: Twin Rivers 96, east wall solution cavity)

This specimen is a sub-rounded pebble 4cm across, with an irregular surface corresponding to significant internal porosity. The cut specimen shows pale crystals within the dominant haematite, and these are almost certainly quartz, but unfortunately none appeared within the examined section.

This specimen shows a relict texture preserved by varying density and size of haematite crystallites. The chemical analysis shows this specimen to be almost pure haematite. The relict grains are angular, show a well defined rim overgrown by radially oriented haematite (Figure 1o-p). Inside, the grains show a slightly more porous fine-grained haematite. The centres of the grains may be formed of the less porous haematite, like the overgrowths, some times with preserved void space at the centre of the original grain. In some cases the fill occluding this pore space is a specularite with crystals of haematite up to 100µm in length (Figure 1q).

Description of the matrix of the breccia

The breccia has a fine grained matrix which has a brownish colour; this lead to its investigation within the examination of the ferruginous materials. However, the colour does not reflect a high iron content, but rather this material is highly phosphatic.

The polished block (Figure 1r-s) shows that the clastic component of the sediment includes subrounded to well rounded quartz and feldspar grains of up to 500µm (more usually 150µm). Iron oxides and ilmenite are also abundant, but mainly at a finer grain size. The sediment also includes abundant irregular and rounded particles of an apatite, which has a high backscatter coefficient. Voids within the sediment bear botryoidal fringing phosphatic cements with a fibrous microstructure (Figure 1t), followed by calcite.

Geochemistry

	SiO_2	Al_2O_3	Fe_2O_3	MnO	MgO	CaO	Na_2O	K_2O	TiO_2	P_2O_5	LOI	*total*
TR1	9.31	3.22	72.58	0.38	0.34	0.19	<	0.24	0.36	0.68	14.60	*101.91*
TR2	10.01	0.67	83.21	0.09	0.14	0.54	<	0.08	0.23	0.39	5.55	*100.90*
TR3	1.64	1.83	94.85	0.40	0.01	0.12	<	0.02	0.04	0.04	1.70	*100.65*
TR4	2.80	0.48	99.08	0.01	<	0.05	<	0.06	<	0.03	0.89	*103.41*
TR5	*nd*	*nd*	*nd.*	*0.03*	*0.12*	*0.28*	*nd*	*nd*	*0.11*	*0.24*	*nd*	*nd*
TR6	20.38	3.91	2.72	0.57	0.69	32.07	0.16	1.00	0.25	19.33	17.96	*99.05*

Table 1: major element chemistry in wt% determined by XRF (values for TR5 based on ICP-MS analysis). Nd = not determined, < = below detection.

The major element analyses by XRF (Table 1) show a reasonably good approach to a 100% total. The exception (TR4) is just a little high, which is due to calibration problems when Fe_2O_3 is at such extreme values. TR1, in contrast, shows a high loss on ignition (LOI) of 14.6%, indicating the iron minerals are hydrated as well as water being contained elsewhere in the material (if the Fe_2O_3 were all goethite and lepidocrocite the expected LOI would be 7.3%). It is possible therefore that the specimen includes some hydrated gel material. The LOI for TR2 indicates that specimen is a mixture of hydrous and anhydrous iron oxides. The LOI is very low for TR3 and TR4 suggesting they are relatively pure haematite.

TR1 shows a moderate concentration of elements other than iron, consistent with the detrital materials observed petrographically. TR2 shows a high SiO_2 content, corresponding to the observed abundance of quartz. TR3 and TR4 are both relatively pure haematite, and therefore show very high iron contents, extremely low phosphate, very low loss on ignition and low silica and alumina. They differ in TR3 being more aluminous, corresponding to the significant quantities of alumina and kaolinite observed in the pore spaces. TR6 shows elevated phosphate and calcium contents, corresponding to a francolite content of approximately 55%.

Concentrations of trace elements (Table 2) are typically rather low in the iron ores, and the lack of correlation between the various samples reinforces the disparate nature of their petrology.

Figure 2 shows the upper crust-normalised REE profiles for the iron ore specimens. The dissimilarity between the specimens is again apparent:

TR1 shows elevated heavy REE (HREE) contents, with progressive relative depletion towards the light REE (LREE). The sample shows a very slight positive Ce anomaly.

TR2 shows low REE contents, with the HREE present at a steady value of approximately 0.26 of average upper crust levels. The LREE show progressive depletion below this level, with a marked negative Ce anomaly.

TR3 shows REE contents generally around 0.1-0.2 of average upper crustal levels, with a somewhat humped profile, with Eu_N reaching 0.3 (although may be somewhat exacerbated by interference with the significant Ba content of this sample). The LREE have normalised values of approximately 0.13-0.14, upon which is superimposed a large positive Ce anomaly.

TR4 shows a somewhat similar profile to TR2, with slightly higher REE contents, and a slight relative depletion of the HREE. The negative Ce anomaly I more marked than that of TR2.

TR5 shows very low REE contents, and many elements fall below the detection limits. The LREE show a small positive Ce_N anomaly. The few heavier REE detectable show a relative depletion towards the REE. The overall profile is probably closest to TR3.

The upper crust-normalised REE profile for TR6 (Figure 3) is only very slightly humped, and is therefore typical of fine-grained sediment. The profile suggests that the sediment source is a primary source, and the sediment has not been recycled through lateritic deposits.

Conclusion and suggestions for future study

The iron ores recovered from the site include material derived from both laterites and probable vein mineralisation. The mineralised samples are themselves rather variable and may not necessarily represent a single source. It is safe to say that only one of the four is a typical laterite – the other three are probably derived from other, older, geological sources. However, the variability present does not permit determination of whether they derive from a single variable source, or (more likely the case) that they derive from several distinct sources.

Two of the iron ore specimens (TR1, TR3) bore a brown ferruginous crust, and the other two (TR2, TR4) had very dark, smoothed outer surfaces. This suggests that the materials were derived pebbles, and not materials obtained fresh at outcrop. One aim of future investigations should be to determine whether any superficial deposits in the area contain derived iron ores.

The two replacement ores are texturally dissimilar. TR2 shows relict polygonal grain boundaries picked out by discontinuous rims of quartz, discontinuous rims of dense haematite, euhedral neomorphic quartz crystals (with intergrown haematite) and by cracking. In contrast TR4 shows angular replaced grains with a low-density of haematite crystals, overgrown with more dense haematite crystals which become specularite in voids. The two samples share some similarities in their chemical compositions, including their upper crust-normalised REE profiles, but TR2 has elevated levels of most trace elements compared with TR4 (except for U, Mo, Sr, Ge).

The specularite sample (TR3) is marked by an open texture of large haematite crystals. Some of the void space is filled by aluminous material, including kaolinite, an alumina mineral (?bauxite), fine-grained Al, Si, Fe bearing clay and a fine-grained Mn, Al mineral possibly a spinel. The upper crust-normalised REE profile differs from all the other specimens, with a large positive cerium anomaly.

Determination of the nature of the ochreous residue on the hammerstone (TR5) was one of the main aims of the work. Sampling of the ochre will inevitably have involved some contamination from the hammerstone itself. This leads to uncertainty in the interpretation, given that the ochre does not have a very close chemical resemblance to any of the lump ore types. The ochre was present in only a very small quantity, so major element analysis was not possible. The REE profile hints at a similarity to that of the specularite (TR3), but low concentrations of the REE precludes detailed comparison of the profile. Some of the other elements (e.g. Th being present in significantly greater quantities than U) suggest comparison with quartz-rich replacement ore (TR2). Other elements again (particularly the metals V, Cu, As, Pb) are present in much higher concentrations in TR2 than in the ochre. There are no suggestions in the chemical analyses that the ochre was derived from the laterite. Until some evidence for the spectrum of possible sources of replacement ores/specularites becomes available (and for the compositional range within each source) it will not be possible to refine the provenancing of the ochre any more closely, than to say that it is unlikely to have been produced from laterite alone.

The matrix of the breccia (TR6) proved to contain little iron (despite its colour). The material proved to be dominated by phosphate minerals, probably representing material reworked from bat droppings.

The attempt to cut material from the block with cut marks (TR7), failed to produce any usable specimen, because the soft rock crumbled on cutting. The attempt to identify the rock type by this root was abandoned to avoid causing any more damage to the specimen. However, the attempt did reveal the presence of a weathered crack corresponding to one of the grooves on the opposing face, confirming the proposition that the grooves are natural weathering features.

The cutting of a clast from the breccia (TR8) to examine whether the carbonate rocks contained any fine-grained iron oxides which might be the source of the ochre demonstrated that, in this clast at least, there was no included iron oxide material which could be liberated on weathering.

Zambian geology includes numerous distinct occurrences of specularite of different ages and host stratigraphic horizon. Detailed consideration of the solid geology close to the site may reveal potential sources. It is unlikely that any detailed trace element analyses of such occurrences will have been made previously, and there may not even be published petrographic textures. Any further attempts to refine the provenancing of the samples is likely to require fresh collection of the possible sources. Given the possiblity that the materials are derived pebbles, then the ultimate geological source may not necessarily be the immediate provenance, but rather they may derive from secondary deposits.

Figure 1.

Backscattered electron photomicrographs of polished samples from Twin Rivers.

a-f. TR1
a.-b. areas rich in surviving detrital minerals. Grains are dominantly quartz, but K-feldspar (lower right (a)), mica (e.g. biotite lower left of centre (a)), spinels and phosphates also occur.
c. area poor in detrital grains, apart from mica (right centre). Matrix shows patchy distribution of material with differing backscatter coefficients.
d. Detail of area with high backscatter coefficient, showing very small monazite grains in haematite.
e. Coated ferruginous grains.
f. Detail of superficial coating on pebble, showing penetration into cracks in pebble.

g-j. TR2
g. low magnification view showing polygonal network representing grain boundaries of replaced texture.
h. neomorphic euhedral quartz with intergrown haematite.
i. detail showing variable development of haematite and quartz on former grain boundaries.
j. Internal structure of some replaced grains defined by concentric voids (picked out in this image through the influence of secondary electrons).

k-n. TR3
k. low magnification view of specularite texture.
l. detail of area at bottom left of (k) shoeing porosity filled by alumina minerals and kaolinite.
m. detail of area on left of void showing specularite (white) overgrown by a second generation normal to platelet surfaces, in turn overlain by a Mn, Al-bearing mineral, possibly galaxite (mid grey). Dark grey areas include various aluminosilicates and alumina minerals (very dark).
n. Region of specularite showing a coarser scale structure in platelet orientation.

o-q. TR4
o-p. low magnification views showing void space, angular grains replaced by haematite (picked out by differing density of crystallites).
q. specularite occurrence in centre of replaced grain.

r-t. TR6
r. low magnification view showing poorly sorted sediment and porespace occluded by cement.
s. pore with phosphate (zoned) and calcite cements. Sediment shows well-rounded grains of quartz, K-feldspar, apatite, ilmenite, which may show some corrosion, set in a matrix which is heavily phosphatised.

	Li	Be	Sc	V	Cr	Cu	Zn	Ga	Ge	As	Rb	Sr
TR1	10.41	15.67	17.08	316.51	123.98	22.43	119.71	13.46	1.62	127.80	4.95	14.26
TR2	1.86	0.37	1.50	477.15	22.09	404.27	158.52	2.82	2.07	59.12	4.27	6.75
TR3	15.86	0.34	0.55	20.58	4.70	58.63	17.60	1.85	1.21	2.62	2.58	9.13
TR4	1.52	4.10	5.81	30.42	2.22	5.50	4.80	3.00	37.97	11.22	7.36	10.13
TR5	<	<	<	23.08	28.02	81.52	129.66	2.33	1.21	<	10.24	8.48
TR6	14.94	1.01	4.55	38.75	37.32	32.87	122.47	5.87	0.59	<	45.14	136.76

	Y	Zr	Nb	Mo	Cd	Cs	Ba	Tl	Pb	Bi	Th	U
TR1	44.08	95.07	8.83	11.31	0.26	0.12	188.96	0.15	5.06	0.87	3.93	4.18
TR2	6.22	33.74	4.08	1.96	<	0.11	87.57	<	178.59	0.91	1.32	0.68
TR3	3.02	5.95	1.30	4.87	<	0.18	295.29	0.21	28.23	0.84	0.65	2.20
TR4	5.68	6.40	0.53	8.77	<	0.70	32.66	<	13.26	0.70	0.42	9.17
TR5	1.59	33.07	1.84	<	<	0.51	54.96	<	13.39	<	1.40	0.50
TR6	11.26	49.10	5.00	0.57	<	1.10	652.37	0.23	7.83	0.23	4.21	1.55

	La	Ce	Pr	Nd	Sm	Eu	Gd	Tb	Dy	Ho	Er	Tm	Yb	Lu
TR1	20.74	55.83	3.39	12.50	3.21	0.96	4.03	0.74	5.50	1.37	4.98	0.89	6.59	1.18
TR2	5.16	5.60	1.29	5.12	1.06	0.25	1.09	0.18	1.03	0.21	0.56	0.09	0.59	0.07
TR3	4.35	62.91	0.91	3.21	0.62	0.27	0.95	0.11	0.62	0.09	0.26	0.04	0.18	0.03
TR4	14.31	12.39	3.92	12.88	2.72	0.54	2.27	0.34	1.85	0.26	0.74	0.11	0.88	0.12
TR5	3.39	10.03	0.72	<	<	<	<	0.07	<	<	0.14	<	<	*(0.06)*
TR6	17.00	31.59	3.77	13.91	2.68	0.71	2.61	0.38	2.16	0.40	1.12	0.16	0.97	0.15

Table 2. Trace element chemistry in ppm, determined by ICP-MS (elements also determined by XRF excluded). < = below detection.

TR1: TR96 Block F limonite

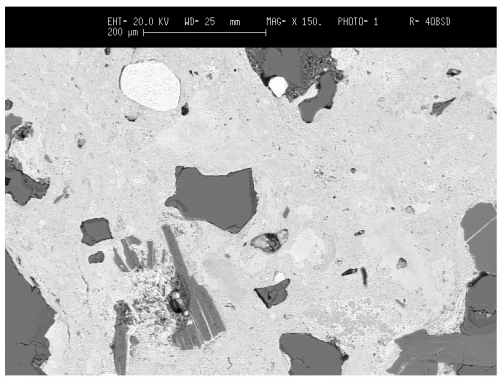

a

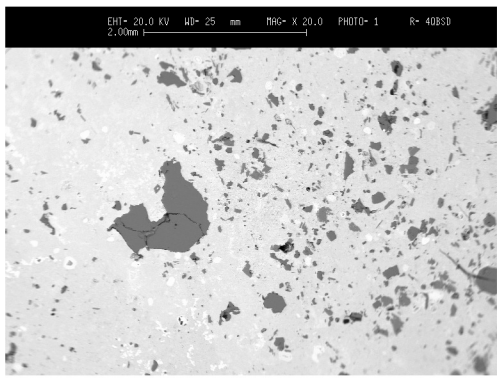

b

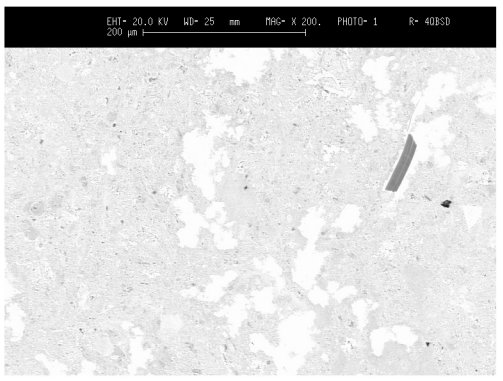

c

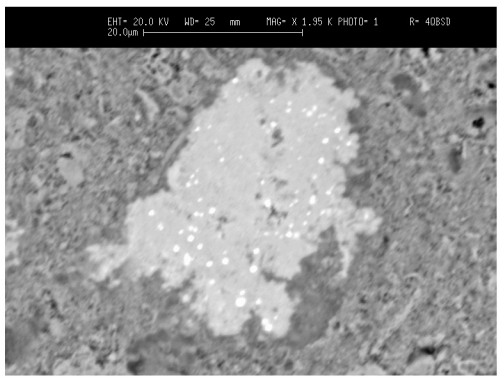

d

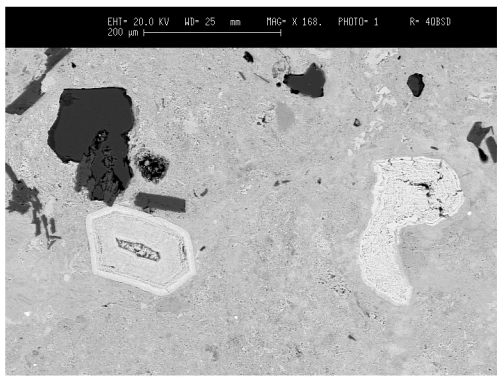

e

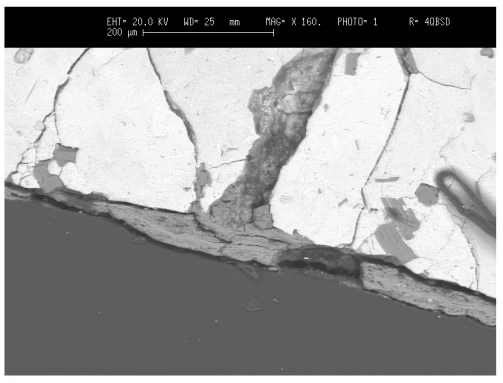

f

TR2: laterite #2 (brown)

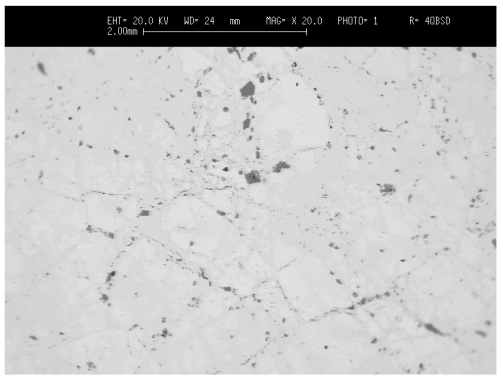

g

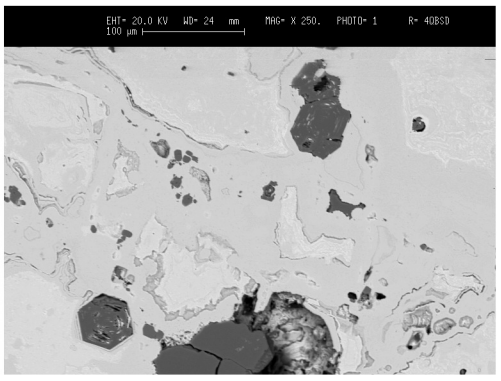

h

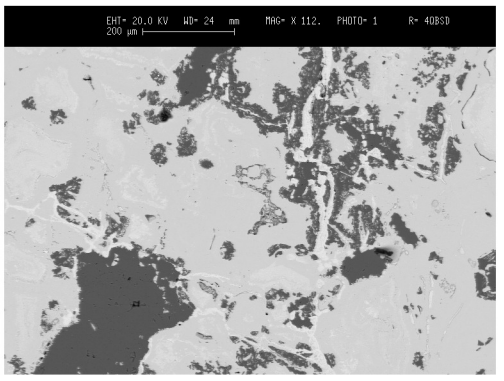

i

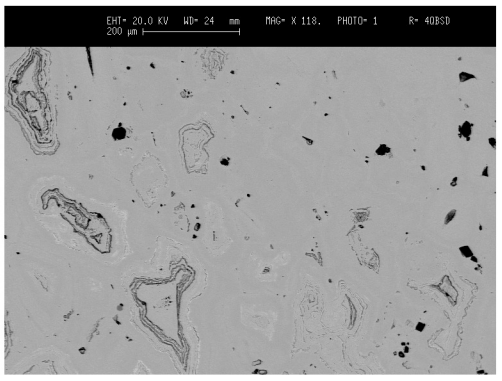

j

TR3: laterite #3 (specularite)

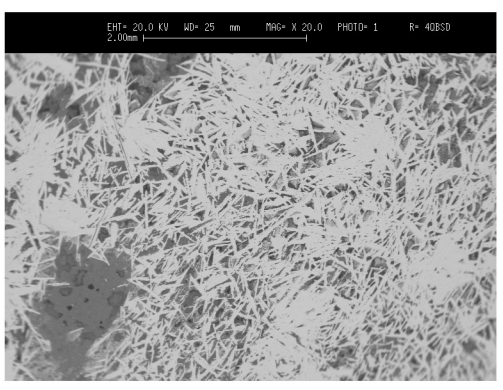

k

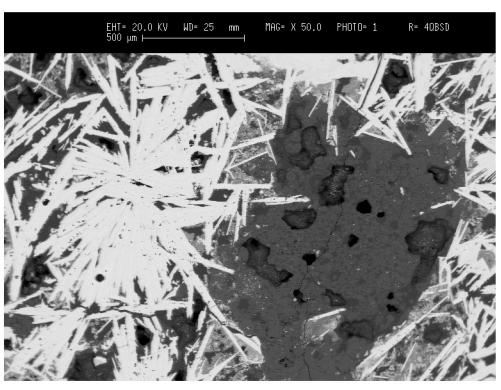

l

m

n

TR4: laterite #4 (red, specularuite in voids)

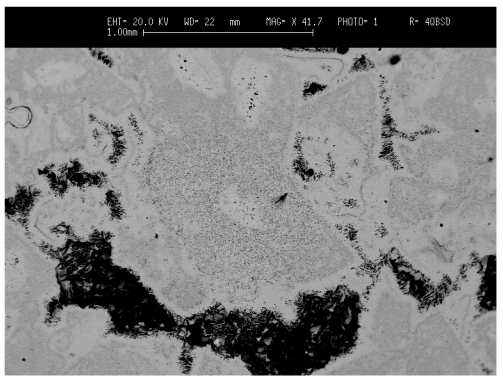

o

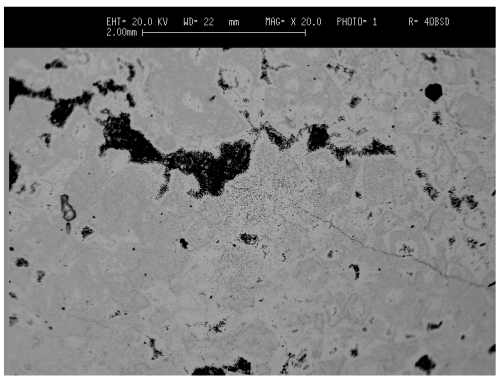

p

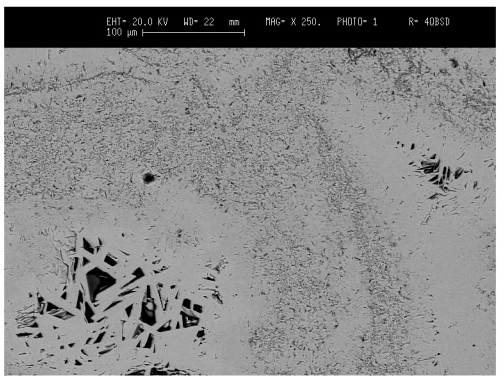

q

TR6: matrix from breccia

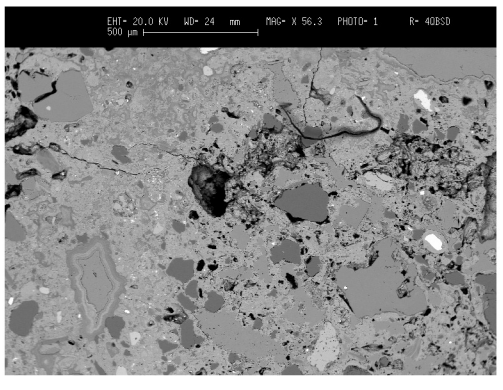

r

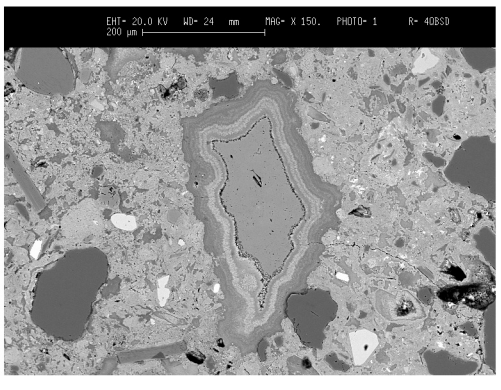

s

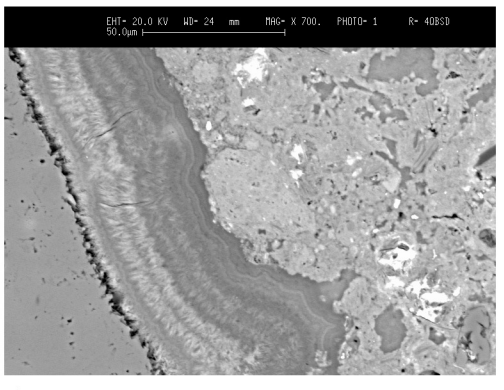

t

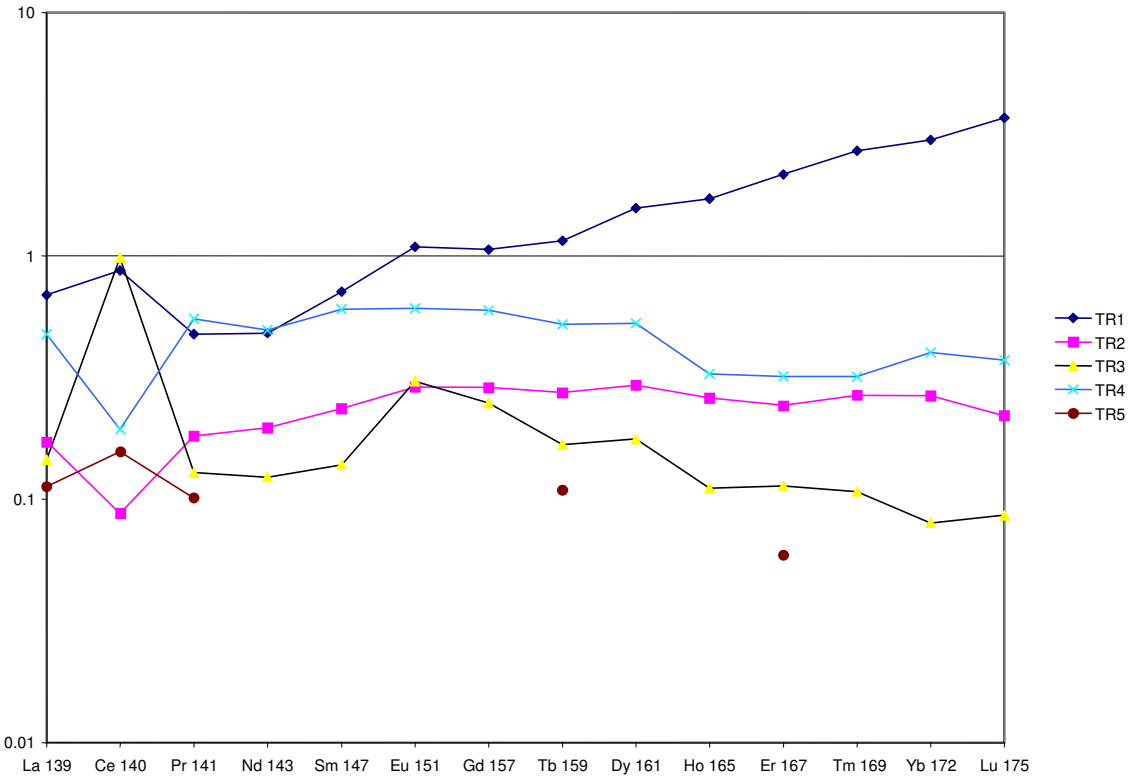

Figure 2. Upper crust normalised REE profiles (normalisation factors after Taylor & MacLennan 1981) for the iron ore specimens.

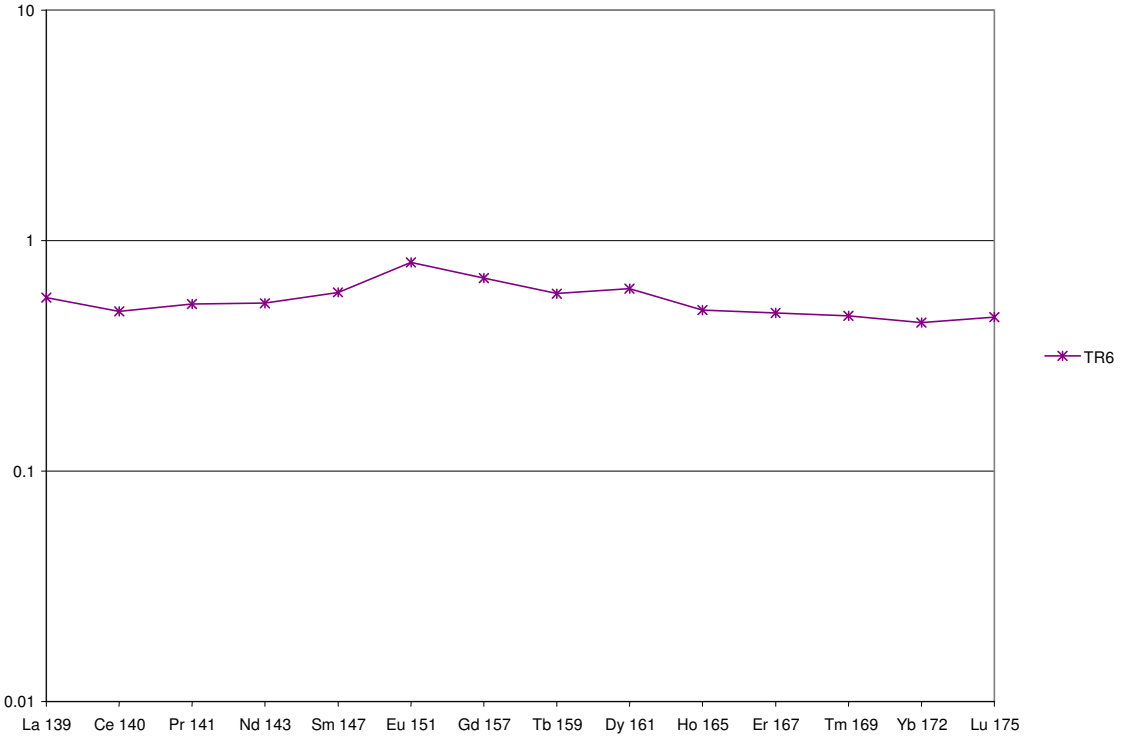

Figure 3. Upper crust normalised REE profiles (normalisation factors after Taylor & MacLennan 1981) for the matrix of the breccia (TR6).